A Switched Extremum Seeking Approach to Maximum Power Point Tracking in Photovoltaic Systems

by

Scott Moura

sjmoura@umich.edu

EECS 498-003 Project

Grid Integration of Alternative Energy Sources

Professor Ian Hiskens

April 21, 2009

Contents

1 Introduction

This project examines a switched extremum seeking approach for determining the maximum power point of a photovoltaic (PV) system, using DC/DC converter power electronics (Fig. 1). The proposed switched extremum seeking controller leverages averaging and Lyapunov stability theory to converge to the maximum power point asymptotically. This concept is demonstrated through simulation, using mathematical models for PV cells and DC/DC converters introduced in class.

Solar energy represents a key opportunity for increasing the role of renewable energy in the electric grid. However, high manufacturing and installation costs have limited the economic viability of PV-based energy production [1]. Therefore, it is vitally important to maximize the energy conversion efficiency of PV arrays. This problem is particularly difficult because high fidelity PV models require detailed semiconductor physics, which are highly dependent on environmental conditions, such as incident solar radiation, temperature, and shading effects. As such, we require control theoretic techniques that mathematically guarantee asymptotic convergence to the maximum power point, while rejecting disturbances due to changing environmental conditions.

The MPPT literature is extremely broad, and contains techniques that range in complexity, sensor requirements, convergence speed, implementation hardware, and popularity, among other characteristics. A recent review paper by Esram and Chapman provides a comprehensive comparative analysis of several techniques, summarizing over 90 publications [2]. Several of the most popular methods can be broadly classified into three categories: feedforward look-up tables [3–5], perturb and observe (P&O) methods [6, 7], and the incremental conductance (IncCond) approach [8]. Further interested readers should refer to the review paper [2] and references therein for a more expansive analysis of MPPT techniques. The feedforward approach uses experimental PV characteristic data to build functions that map operating conditions, such as temperature and incident solar flux, to the maximizing voltage input. These approaches often use neural networks [3, 4] or fuzzy logic techniques [5]. The P&O method perturbs the input voltage to determine the direction of the maximum power point, and moves the operating point accordingly. For example, if voltage is increased and the measured power output increases, the voltage is set to increase further until measured power decreases. At this point, the controller enters a periodic orbit about the maximum power point. This approach does not require *a priori* knowledge of the PV system and is very simple to implement. However, P&O can diverge from the maximum power point under certain variations in the environmental conditions [6,7]. An alternative method, incremental conductance, seeks to correct this issue by leveraging the fact that the slope of PV array power output is zero at the maximum power point. As a result, this algorithm estimates the slope of the power curve by incrementing the terminal voltage until the estimated slope oscillates about zero [8]. A drawback of P&O and IncCond methods is that both methods enter limit cycles about the maximum power point rather than converging to it exactly. If the PV characteristics are known beforehand,

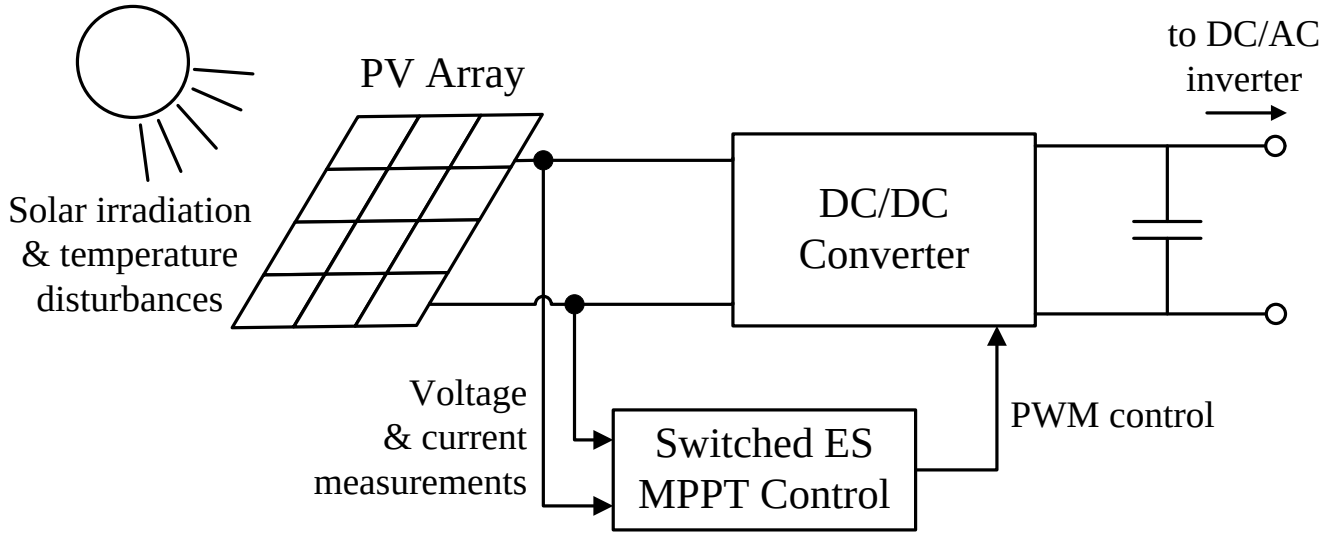

Figure 1: PV system, including a PV array, DC/DC converter, switched ES MPPT control.

the feedforward approaches reach the maximum power point exactly. However, experimental data and physical models are typically subject to uncertainty and external disturbances. Therefore it is desirable to obtain a peak seeking scheme that is asymptotically convergent and is self-optimizing with respect to shifts in the maximum power point. This motivates a control-theoretic approach to MPPT, namely extremum seeking. This project report makes the following two new contributions to the MPPT literature. First, we examine the applicability of extremum seeking for MPPT in photovoltaic systems, a method developed from a control-theoretic basis. Second, we introduce a modification to the traditional extremum seeking approach that eliminates limit cycles and allows asymptotic convergence, using averaging and Lyapunov stability theory. We call this algorithm "switched extremum seeking." Although this report applies switched extremum seeking to MPPT in photovoltaic systems, the algorithm is general and can be applied to a wide variety of applications (e.g. air flow control in fuel cells [9], wind turbine energy capture [10], and ABS control [11]).

This report is organized as follows: Section 2 develops models for the PV array system and DC/DC converter power electronics. Section 3 introduces the extremum seeking algorithm, analyzes the stability proof, and proposes the switched approach that allows asymptotic convergence. Section 4 evaluates the proposed switched extremum seeking controller and the impact of varying environmental conditions through simulation. Finally, Section 5 contains the key conclusions of this report.

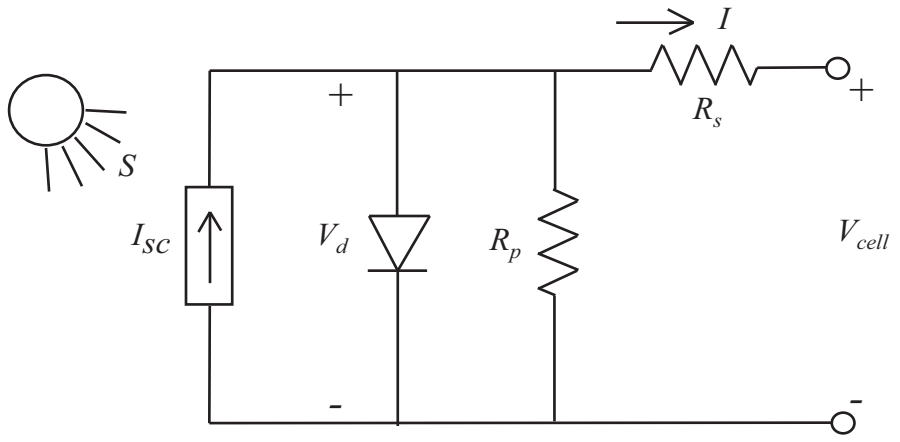

Figure 2: Equivalent circuit model of PV cell.

2 PV System Model Development

2.1 Equivalent Circuit PV Array Model

For the purposes of MPPT we consider an equivalent circuit model of a photovoltaic cell, adopted from [12] and shown in Fig. 2. This model consists of an ideal current source I_{lg} in parallel with a diode and parallel resistance R_p. Together, these elements are in series with another resistor R_s, which models the resistance in the contactors and semiconductor material. The ideal current source delivers current in proportion to solar flux S, and is also a function of temperature T. The diode models the effects of the semiconductor material, and is also a function of temperature[1]. In total, the PV cell model equations are given by

$$V_d = V_{cell} + IR_s \tag{1}$$

$$I = I_{sc} + I_0(e^{\frac{qV_d}{AkT}} - 1) - \frac{V_d}{R_p} \tag{2}$$

$$I_{sc} = (I_{sc,r} + k_I(T - T_r))\,\frac{S}{1000} \tag{3}$$

$$I_0 = I_{0,r}\left(\frac{T}{T_r}\right)^3 \exp\left(\frac{qE_{Si}}{Ak}\right)\left(\frac{1}{T_r} - \frac{1}{T}\right) \tag{4}$$

$$V = n_{cell}V_{cell} \tag{5}$$

The PV cell model is scaled to represent a PV array by considering 36 cells arranged in series, as described by (5). Since (1)-(2) are nonlinear functions of cell current I and voltage V_{cell}, they must be solved numerically, using Newton's algorithm for example. The parameters for this model are adopted from [12] and provided

[1]The temperature dependent equations for short-circuit and reverse diode saturation current (3)-(4) are necessary to accurately capture the impact of temperature. These equations augment the PV cell model presented in class and the textbook by Masters [13]

in Table 1.

The PV model is parameterized by environmental conditions - namely incident solar irradiation S and temperature T. Figure 3(a) demonstrates that current and power increases linearly with incident solar irradiation. Figure 3(b) demonstrates that temperature has a more complex impact on current and power. The short circuit current increases slightly with temperature, however the power (and the maximum power point) decreases as temperature increases. In other words, PV cells operate best in full sunlight and cold temperatures. As a result of these characteristics, it is critical to develop a control loop that automatically tracks the maximum power point under varying environmental conditions, so as to maximize energy conversion. This will be the focus of the remainder of the report.

2.2 DC/DC Boost Converter

A DC/DC boost converter steps up the PV array voltage and provides a control actuator for MPPT, using PWM control on the switches. At the output end of the boost converter, a capacitor maintains a roughly constant voltage of 120V. This topology is typically interfaced with the electric grid using a three-phase DC/AC inverter, similar to the one described in [7]. In this report, we focus on the boost converter only for the purposes of MPPT, and assume the capacitor maintains a constant 120V at the output. Since the switching frequency is significantly faster than the extremum seeking control loop dynamics, we model the boost converter by the following static relation [14]

$$V = V_{inv}(1 - d) \tag{6}$$

where V is the voltage imposed across the PV array, V_{inv} is the constant 120 V maintained by the capacitor as an input to the inverter, and d is the duty ratio that serves as the control input.

Table 1: Photovoltaic Array Parameters

Parameter	Description	Value
A	Ideality factor	1.92
E_{Si}	Band gap energy for silicon	1.11 eV
$I_{0,r}$	Reference reverse saturation current	20×10^{-6} A
$I_{sc,r}$	Reference short-circuit current	2.52 A
k_I	Short-circuit temperature coefficient	0.0017 A/K
k	Boltzmann's constant	1.38×10^{-23} C
n_{cell}	Number of PV cells arranged in series	36
q	Electron charge	1.6×10^{-19} C
R_p	Parallel resistance	9 Ω
R_s	Series resistance	0.0009 Ω
T_r	Reference temperature	301.18 K

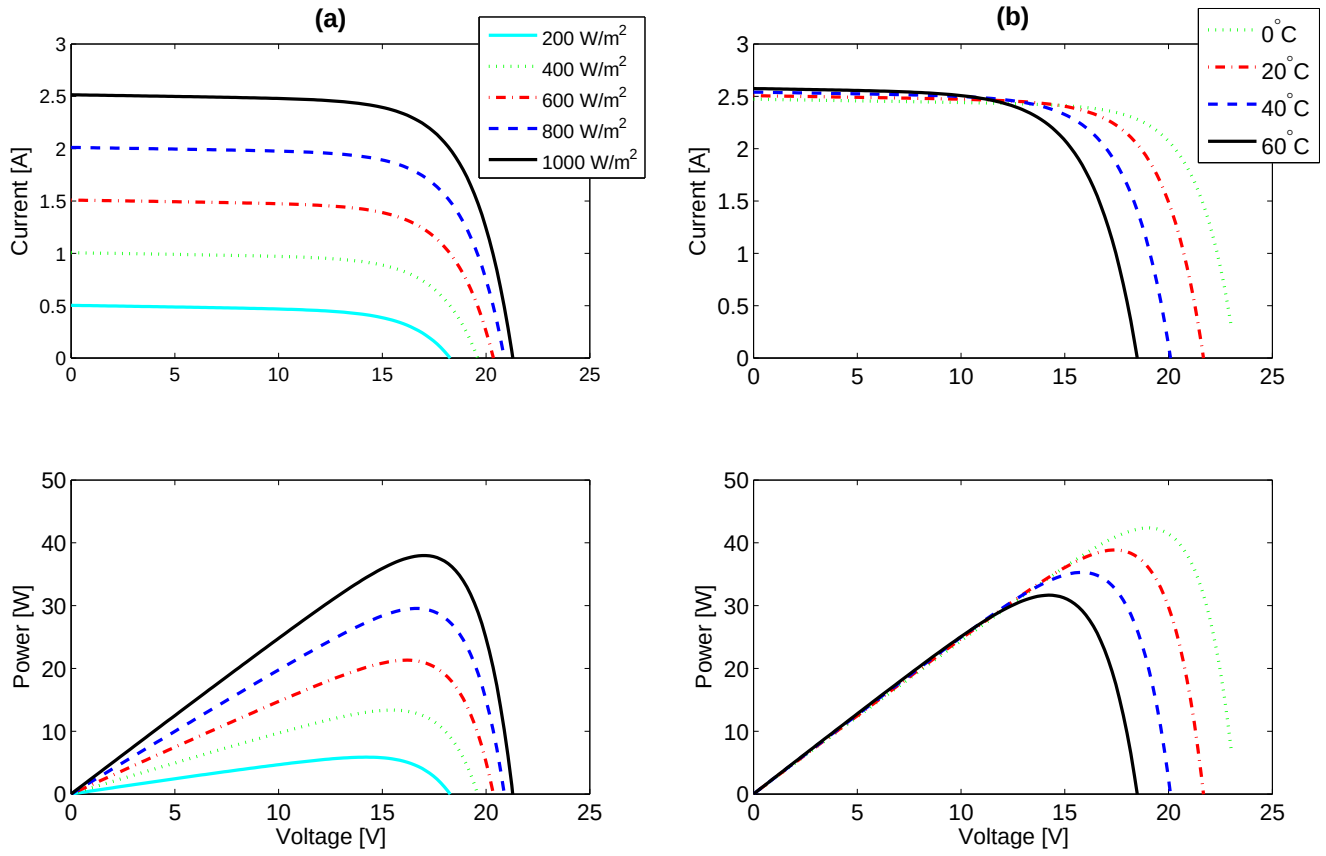

Figure 3: Characteristic I-V and P-V curves for (a) varying irradiation levels and $T = 25°\text{C}$, (b) varying temperature levels and $S = 1000W/m^2$.

3 Extremum Seeking Control

To maximize the PV array power output, we employ a simple yet widely studied extremum seeking (ES) scheme [11,15] for static nonlinear maps, shown in Fig. 4. Before embarking on a detailed discussion of this method, we give an intuitive explanation of how the approach works, which can also be found in [11,15], but is presented here for completeness. Next we discuss the design of the ES feedback loop. Finally, we propose a Lyapunov-based switching scheme that causes the sinusoidal perturbation to decay exponentially once it has converged near the optimum value. If the optimum value shifts, the Lyapunov function will automatically sense the disturbance and re-enable the sinusoidal perturbation to converge to the new optimal value.

3.1 An Intuitive Explanation

The control scheme applies a periodic perturbation $a_0 \sin(\omega t)$ to the duty ratio signal $\hat{d}$, which is the current estimate of the optimum duty ratio d^*. Assuming the DC/DC converter dynamics can be approximated as instantaneous, the sinusoidally varying duty ratio imposes a sinusoidally varying input voltage. This voltage passes through the static nonlinearity $f(\hat{d}+a_0 \sin(\omega t))$, representing the PV array's P-V characteristic curve, to produce a periodic power output p. The high-pass filter $s/(s+\omega_h)$ then eliminates the DC component of p, and will be in phase or out of phase with the perturbation signal $a_0 \sin(\omega t)$ if $\hat{d}$ is less than or greater than d^*, respectively. This property is important, because when the signal η is multiplied by the perturbation signal $\sin(\omega t)$, the resulting signal has a DC component that is greater than or less than zero if $\hat{d}$ is less than or greater than d^*, respectively. This DC component is then extracted by the low-pass filter $\omega_l/(s+\omega_l)$. Therefore, the signal ξ can be thought of as the sensitivity $(a_0^2/2)\frac{\partial f}{\partial d}(\hat{d})$ and we may use the gradient update law $\dot{\hat{d}} = k(a_0^2/2)\frac{\partial f}{\partial d}(\hat{d})$ to force $\hat{d}$ to converge to d^*.

3.2 ES Control Design

The synthesis process for an extremum seeking controller requires proper selection of the perturbation frequency ω, amplitude a_0, gradient update law gain k, and filter cut-off frequencies ω_h and ω_l. The perturbation frequency must be slower than the plant dynamics to ensure the plant appears as a static nonlinearity from the viewpoint of the ES feedback loop. Large values for a_0 and k allow faster convergence rates, but respectively increase the oscillation amplitude and sensitivity to disturbances. Therefore, one typically increases these parameter values to obtain maximum convergence speed for a desirable amount of oscillation and sensitivity, while ensuring time scale separation between the plant and ES feedback loop. The filter cut-off frequencies must be designed in coordination with the perturbation frequency ω. Specifically, the high-pass filter must not attenuate the perturbation frequency, but the low-pass filter should, thus bounding the cut-off frequencies from above. Mathematically $\omega_h < \omega$ and $\omega_l < \omega$. Moreover, the filters should have sufficiently

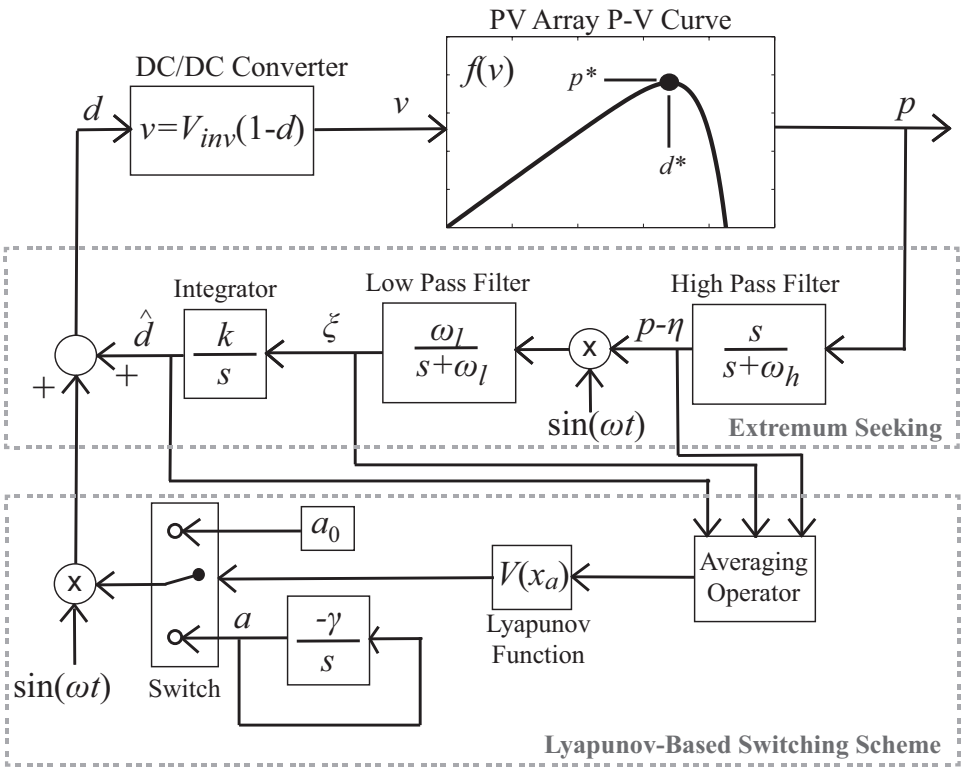

Figure 4: Block diagram of proposed switched extremum seeking control system.

fast dynamics to respond quickly to perturbations in the control input, thereby bounding the cut-off frequencies from below. Generally, proper selection of the ES parameters is a tuning process. However, the above guidelines are extremely valuable for effective calibration. More detailed information on ES parameter design can be found in [9]. The ES parameter values used in this report are provided in Table 2.

Table 2: Extremum Seeking Parameters

Parameter	Description	Value
ω	Perturbation frequency	250 Hz
a_0	Perturbation amplitude	0.015
k	Gradient update law gain	1
ω_h	High-pass filer cut-off freq.	50 Hz
ω_l	Low-pass filer cut-off freq.	50 Hz

3.3 Averaging Stability Analysis

The proposed extremum seeking method, using periodic perturbations, is particularly appealing because it converges to the local optimum of a static nonlinearity in real-time, without *a priori* knowledge of the nonlinearity itself. Moreover, ES is self-optimizing in the presence of rapidly changing environmental conditions, such as irradiation and temperature. However, a general drawback of this method is that once the optimum value is determined, the ES feedback loop causes the system to enter a limit cycle around this value, as opposed to converging to it asymptotically. This issue also occurs in general P&O and IncCond algorithms. To eliminate this limit cycle, we propose a switched control scheme that effectively decays the amplitude of the periodic perturbation once the system has converged within the interior of a ball about the optimum value. The switch-off criterion is determined using Lyapunov stability methods. That is, we leverage a Lyapunov function designed from an averaged, linearized model of the original ES feedback system to estimate the proximity to the equilibrium point[2]. Once the Lyapunov function value falls below some threshold value, the amplitude of the sinusoidal perturbation is passed through an integrator with negative gain, thus producing an exponentially decaying signal. If the Lyapunov function value raises above the switch threshold, due to changing environmental conditions, then the amplitude returns to its original value. The idea of allowing the perturbation to decay exponentially is not new, and has been proposed in [16]. However, this is the first application of an exponentially decaying perturbation for extremum seeking in a switched scheme, to the author's knowledge.

We begin by proving the optimum value of the static nonlinearity is exponentially stable in the average sense. The proof proposed by Krstic and Wang [15] uses averaging theory to develop an averaged nonlinear system, linearizes it about the optimum, and then shows the resulting Jacobian is Hurwitz. From this proof, our new contribution is to develop a Lyapunov function that senses the proximity to the equilibrium point.

The state equations for the closed-loop MPPT PV array system can be written as follows:

$$\dot{\hat{d}} = k\xi \tag{7}$$

$$\dot{\xi} = -\omega_l \xi - \omega_l \eta \sin(\omega t) + \omega_l f(v) \sin(\omega t) \tag{8}$$

$$\dot{\eta} = -\omega_h \eta + \omega_h f(v) \tag{9}$$

$$v = V_{inv}\left(1 - \hat{d} - a_0 \sin(\omega t)\right) \tag{10}$$

where each equation respectively represents the integrator, low-pass filter, high-pass filter, and DC/DC converter dynamics. Note that the DC/DC converter dynamics in (10) are approximated as instantaneous, since the switching frequency for the MOSFETs in the converter is orders of magnitude higher than the ES

[2]The inspiration for this switched controller came from Homework #9 in Professor Jessy Grizzle's EECS 562 Nonlinear Systems and Control course. In this problem set, we use the same concept to stabilize a pendulum on a cart.

loop dynamics. Also recall that V_{inv} represents the voltage input to the DC/AC inverter, which is assumed to be constant.

Now define a new coordinate system that shifts the equilibrium/maximum power point to the origin

$$\tilde{d} = \hat{d} - d^* \tag{11}$$

$$\tilde{\eta} = \eta - f(v^*) \quad \text{where} \quad v^* = V_{inv}(1 - d^*) \tag{12}$$

resulting in the following translated system

$$\dot{\tilde{d}} = k\xi \tag{13}$$

$$\dot{\xi} = -\omega_l \xi + \omega_l \tilde{\eta} \sin(\omega t) - \omega_l f(v^*) \sin(\omega t) + \omega_l f(\tilde{v}) \sin(\omega t) \tag{14}$$

$$\dot{\eta} = -\omega_h \tilde{\eta} - \omega_h f(v^*) + \omega_h f(\tilde{v}) \tag{15}$$

$$\tilde{v} = V_{inv}\Big(1 - \tilde{d} - d^* - a_0 \sin(\omega t)\Big) \tag{16}$$

To investigate the stability properties of this system, we consider the averaged system, as done in [15]. This makes intuitive sense because extremum seeking injects a sinusoidal perturbation into the system to estimate the gradient of the nonlinearity. Therefore the actual behavior should match the averaged behavior. The averaged state variables are defined as follows [17]

$$x_a = \frac{\omega}{2\pi} \int_{t - \frac{2\pi}{\omega}}^{t} x(\tau) d\tau \tag{17}$$

where the period of the signal is $\frac{2\pi}{\omega}$. Hence, our immediate goal is to use the notion of an average system to investigate the stability properties of the closed loop system. Applying the definition of averaging yields the following system

$$\dot{\tilde{d}}_a = k\xi_a \tag{18}$$

$$\dot{\xi}_a = -\omega_l \xi_a + \omega_l \left(\tilde{\eta} \sin(\omega t)\right)_a + \omega_l \Big(\left(f(\tilde{v}) - f(v^*)\right) \sin(\omega t)\Big)_a \tag{19}$$

$$\dot{\eta}_a = -\omega_h \tilde{\eta}_a + \omega_h \left(f(\tilde{v}) - f(v^*)\right)_a \tag{20}$$

where $(\cdot)_a$ denotes the averaging operation given by the definition in (17). To simplify this system, the following properties are useful:

1. $(\sin(\omega t))_a = 0$
2. $(xy)_a \approx x_a y_a$. That is, the average of the product of two state variables is approximately equal to the product of the average of two state variables. This result arises from Fourier series expansion [18]. Note

that $\sin(\omega t)$ can be considered a state variable by augmenting the system dynamics with a second-order oscillator with eigenvalues at $\pm j\omega$.

These properties imply the second term of (19) is equal to zero, and will help us evaluate the third term of (19) and second term of (20). Note that the third term of (19) is not equal to zero due to the nonlinear term.

Let us first evaluate the second term of (19), $\omega_h \left(f(\tilde{v}) - f(v^*)\right)_a$. For ease of notation, define

$$h(\tilde{d} + a_0 \sin(\omega t)) = f\big(V_{inv}(1 - \tilde{d} - d^* - a_0 \sin(\omega t))\big) - f(d^*) \tag{21}$$

The function $h(\tilde{d} + a_0 \sin(\omega t))$ translates the nonlinear P-V characteristic map so the origin is located at the maximum power point. Let us approximate this function by a quadratic equation:

$$h(\tilde{d} + a_0 \sin(\omega t)) \approx b_0 + b_1(\tilde{d} + a_0 \sin(\omega t)) + b_2(\tilde{d} + a_0 \sin(\omega t))^2 \tag{22}$$

This approximation will be used in the remainder of the analysis. Since the origin is located at the maximum power point, $b_0 = 0$, $b_1 = 0$, and $b_2 < 0$. As we shall see later, these conditions are sufficient for proving the maximum power point is exponentially stable. This implies it is not critical that the quadratic approximation is extremely accurate, or the associated coefficients are known exactly. Substituting the quadratic approximation for the translated nonlinear map and applying the definition of averaging yields the following nonlinear system

$$\dot{\tilde{d}}_a = k\xi_a \tag{23}$$

$$\dot{\xi}_a = -\omega_l \xi_a + \omega_l \left(\frac{1}{2} b_1 a_0 + b_2 a_0 \tilde{d}\right) \tag{24}$$

$$\dot{\eta}_a = -\omega_h \tilde{\eta}_a + \omega_h \left(b_0 + b_1 \tilde{d}_a + b_2 \tilde{d}_a^2 + \frac{1}{2} b_2 a_0^2\right) \tag{25}$$

The Jacobian of this system evaluated at the origin is given by:

$$J = \begin{bmatrix} 0 & k & 0 \\ \omega_l b_2 a_0 & -\omega_l & 0 \\ \omega_h b_1 & 0 & -\omega_h \end{bmatrix} \tag{26}$$

The Jacobian is Hurwitz precisely when $b_2 < 0$, which is true if and only if the static nonlinearity is concave. In the case of estimating the minimum of a convex static map, pick $k < 0$ and $b_2 > 0$, and the Jacobian will be Hurwitz. In other words, the extremum seeking approach converges exponentially to both local maxima and minima.

Since the Jacobian evaluated at the equilibrium point is Hurwitz, the averaged system is exponentially stable according to Theorem 4.7 of Khalil [17]. This also satisfies the conditions of Theorem 10.4 of Khalil [17], which states that the original system has a unique exponentially stable periodic orbit about the maximum power point. Therefore, the conclusion is that the extremem seeking control system is stable in the sense that the averaged system converges exponentially to the extremum. We leverage this fact to design the switching criterion, described in the following section.

3.4 Lyapunov-Based Switching Scheme

As a result of linearizing the average system about the maximum power point, we arrive at a Jacobian that approximates the system dynamics near the equilibrium. We now use this Jacobian to develop a quadratic Lyapunov function for the switching control. This is done by solving the following Lyapunov equation for P

$$PJ + J^T P = -Q \tag{27}$$

where Q is taken to be a symmetric matrix, the identity matrix in our case. This results in the following quadratic Lyapunov function

$$V(x_a) = \frac{1}{2} x_a^T P x_a \qquad \text{where} \quad x_a = [\tilde{d}_a \;\; \xi_a \;\; \tilde{\eta}_a]^T \tag{28}$$

which we use for the following switched control law:

$$d(t) = \begin{cases} \hat{d} + a_0 \sin(\omega t) & \text{if} \quad V(x_a) > \epsilon \\ \begin{cases} \hat{d} + a \sin(\omega t) \\ \frac{da(t)}{dt} = -\gamma a(t) \qquad a(0) = a_0 \end{cases} & \text{otherwise} \end{cases} \tag{29}$$

whose conditions are evaluated only when $sin(\omega t)$ is equal to zero, to ensure the control signal remains continuous in time. In switched control systems, proving stability often degenerates into guaranteeing each sub-controller stabilizes the closed-loop system, and the control trajectory remains continuous at the switch time [19]. Intuitively, it is clear that the proposed switched extremum seeking controller is stable, however future work may analyze this using theory developed by Liberzon [20].

This quadratic Lyapunov function estimates how closely the averaged system converges to the maximum power point. That is, $V(x_a) \to 0$ as $x_a \to 0$. Once extremum seeking converges sufficiently close to the maximum power point, the sinusoidal perturbation decays exponentially to zero and the duty ratio control input arrives at the optimal value d^*. If external disturbances cause the Lyapunov function value to increase above the threshold value ϵ, then the original amplitude a_0 is used until the system converges back to

the maximum power point. When the Lyapunov function drops below the threshold, for the second time, the integrator resets to the initial condition $a(0) = a_0$. This switched control approach has the following advantageous properties:

1. The proposed switched control scheme eliminates the periodic orbit which characterizes existing MPPT algorithms, such as perturb and observe [6, 7] and incremental conductance [8]. Instead, it converges exponentially to the maximum power point. This results in greater power output, since the PV array operates precisely at the maximum power point, rather than oscillating around it.

2. The sub-level set $\Omega_c = \{x_a \in R^3 | V(x) \leq c\}$ with $\dot{V}(x) \leq 0$ is positively invariant, meaning a solution starting in Ω_c remains in Ω_c for all $t \geq 0$. In other words, the Lyapunov function will be decreasing monotonically in time, therefore eliminating the chance for any chattering behavior.

3. Under external disturbances, such as shading, solar irradiation, or temperature shifts, the states x_a shift away from the origin and produce an instantaneous increase in the Lyapunov function value. This causes the sinusoidal perturbation to turn on, and extremum seeking proceeds to find the new maximum power point. That is, the proposed switched control scheme is self-optimizing with respect to disturbances. This situation is illustrated in the following section.

4 Simulation Results & Discussion

In this section we demonstrate the proposed switched extremum seeking MPPT control approach and the impact of varying solar irradiation. Specifically, we impose 1000 W/m^2 or solar irradiation during the first 200ms, and then provide a step change of 500W/m^2 for the next 200ms. This situation might model the transient effect of a cloud blocking the incident sunlight. In these simulations, the duty ratio is initialized at a nominal value of 0.9. We also briefly discuss the implementation benefits and issues of the proposed algorithm.

4.1 Impact of Varying Environmental Conditions

Figure 5 demonstrates the current and power trajectories superimposed on the PV array's characteristic I-V and P-V curves ($S = 1000$ W/m^2). These plots demonstrate that ES indeed achieves the maximum power of 38W at voltage and current values of 17V and 2.24A for $S = 1000$W/m^2, and maximum power of 19.5W at voltage and current values of 18V and 1.09A for $S = 500$W/m^2. Moreover, one can see how the operating point jumps from the 1000 W/m^2 I-V and P-V curves to the characteristic curves for 500 W/m^2. This is due to the step change in incident solar irradiation. Immediately after the step change, the operating point

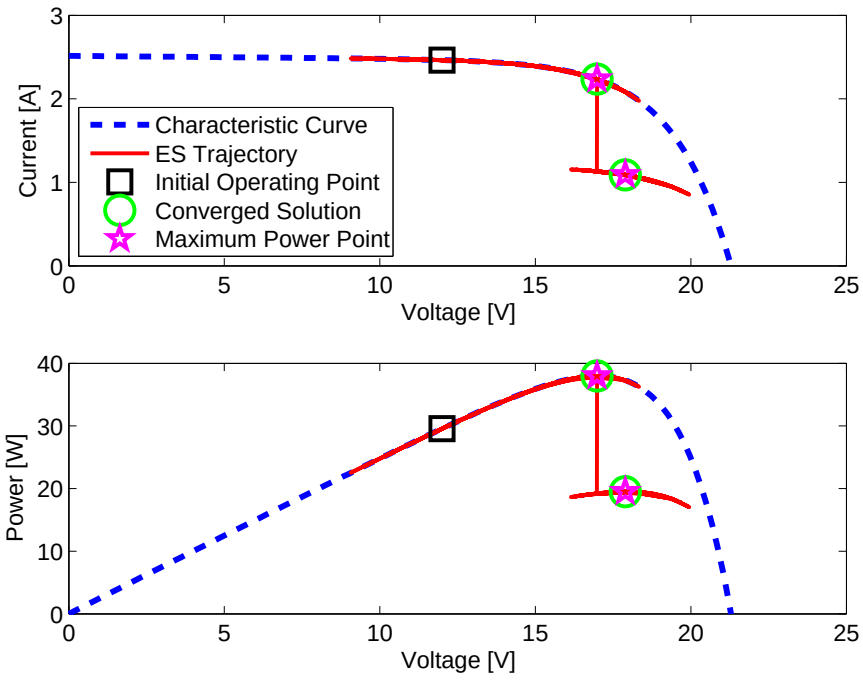

Figure 5: Trajectories of current and power on PV array characteristic curves for 1000W/m^2 to 500W/m^2 step change in solar irradiation.

is no longer at the maximum power point. The switched ES scheme senses this change and then begins to re-optimize to find the new maximum power point.

The time responses of current, voltage, duty ratio, and power are provided in Fig. 6. This figure demonstrates how ES injects sinusoidal perturbations into the duty ratio to determine the maximum power point, which occurs at a duty ratio of 0.8585 for $S = 1000\text{W/m}^2$ and 0.8509 for for $S = 500\text{W/m}^2$. Also observe that the sinusoidal perturbations begin to decay exponentially at 36.5 ms, and the duty ratio converges to the optimal value. Once the irradiation changes at 200 ms, the sinusoidal perturbation re-engages to search for the new maximum power point. Once it converges sufficiently close to the optimal duty ratio, the perturbation amplitude decays exponentially once again.

The switching behavior can be understood by analyzing the Lyapunov function value and switching threshold in Fig. 7. At 36.5 ms, the Lyapunov function crosses over the switching threshold, and thus the amplitude of the sinusoidal perturbation begins to decay exponentially. Once the solar flux step change occurs at 200 ms, the averaged states become excited and the Lyapunov function value exceeds the switching threshold. This resets the amplitude of the sinusoidal perturbation to the original value a_0. Then, as the Lyapunov function value vanishes below the switching threshold, the amplitude of the sinusoidal perturbation decays exponentially once again.

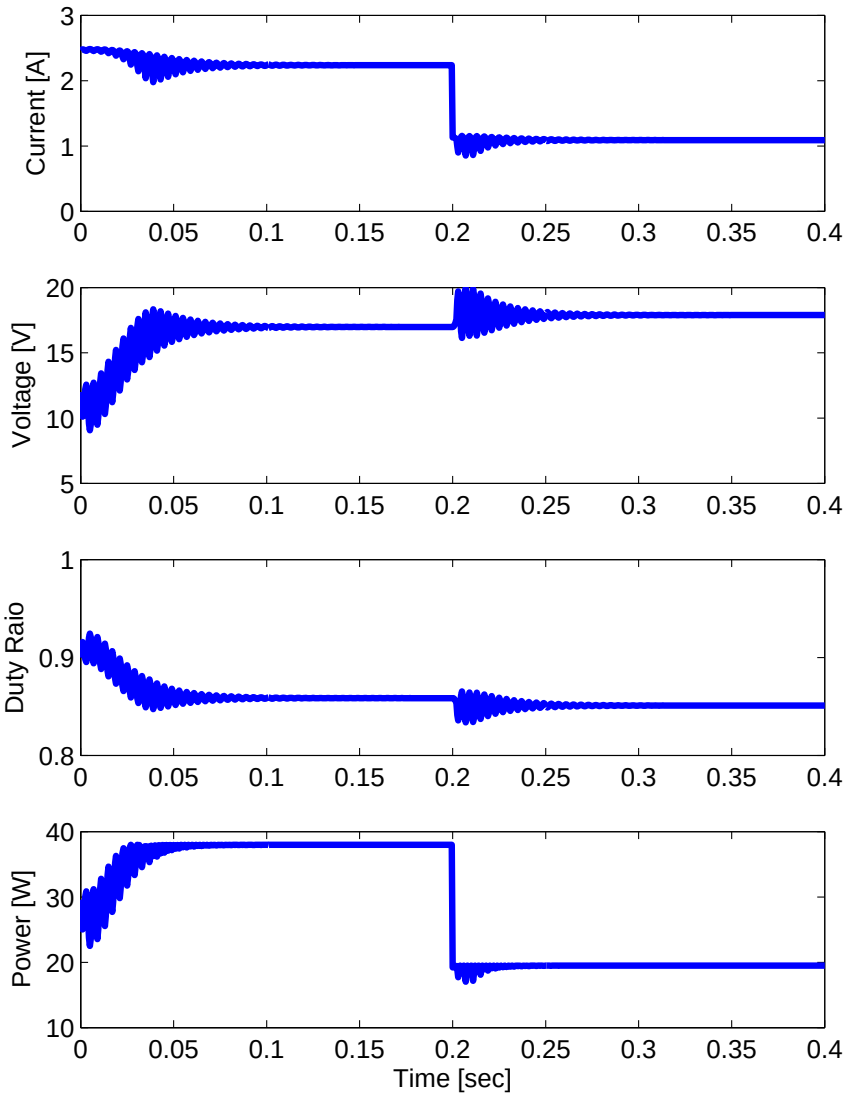

Figure 6: Time responses of PV array current, voltage, duty ratio, and power for 1000W/m^2 to 500W/m^2 step change in solar irradiation.

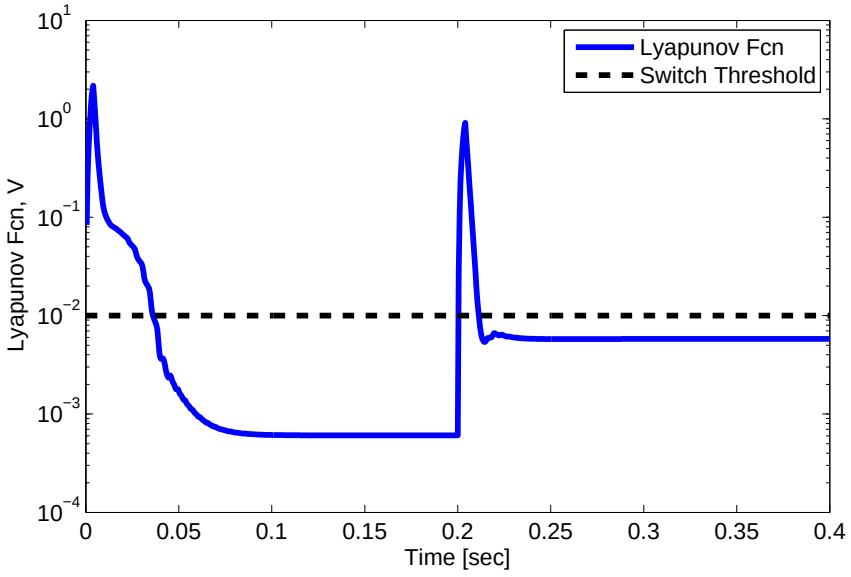

Figure 7: Lyapunov function and switch threshold for 1000W/m^2 to 500W/m^2 step change in solar irradiation.

4.2 Implementation

To this point, we have demonstrated a switched extremum seeking approach to MPPT through theory and simulation only. As such, it is worth noting several advantages and drawbacks to this method with respect to implementation. Overall the switched ES approach has the following implementation advantages over classical MPPT methods:

- Independent of specific PV array characteristics
- Converges asymptotically (exponentially, in fact) to the true maximum power point
- Does not require periodic tuning
- Convergence speed, controlled by appropriate selection of the ES parameters (see Section 3.2), is limited only by the bandwidth of the sensors.
- Requires only voltage and current sensors, which typically exist on PV array systems already.

However, the switched ES approach is also notably more complex than, say, P&O and IncCond techniques. This fact is evident by the block diagram shown in Fig. 4. Besides the computational power required for the ES filters, switching logic, and averaging operator, one also needs to appropriately design the ES parameters and switching threshold. This is an iterative process that can be performed in simulation, but requires some basic knowledge of control systems. That said, the aforementioned issues are typical tradeoffs associated with the application of control-theoretic methods over heuristic algorithms.

5 Conclusions

In this project, we propose a switched extremum seeking control method for maximum power point tracking in a photovoltaic system, controlled via a DC/DC converter. The advantage of the proposed approach over existing methods, such as perturb and observe and incremental conductance, is that the algorithm converges to the optimal power point asymptotically without entering a limit cycle. This fact is proven mathematically using Lyapunov stability and averaging theory. Moreover, the extremum seeking method is self-optimizing with respect to disturbances, such as varying solar irradiation and temperature shifts. Finally, the algorithm is computationally efficient and simple to implement in an experimental system, albeit more complex than typical P&O and incremental conductance methods. The algorithm is developed using PV cell and DC/DC converter models discussed in class, and leverages the author's previous experience in extremum seeking control [9].

The work reported in this project can potentially be extended in the following important and interesting directions:

1. Evaluate the impact of partial shading on each control algorithm. As reported by [21], partial shading typically produces multiple local maximum power points. Since extremum seeking uses a gradient search concept, it will theoretically converge to the local optimum. Hence, further work may be performed to adapt the proposed algorithm to find the global maximum power point, thereby increasing the energy conversion efficiency.

2. Use theory on switched systems [20] to prove the switched closed loop system is asymptotically stable. In the process, we may discover an improved switching controller.

3. Investigate alternative perturbation signals. In this work, sinusoidal perturbations are selected since they are relatively simple to analyze mathematically. However, alternative choices may improve convergence speed [22] or, more importantly, take advantage of perturbations inherent to the physical system. For example, one could leverage the ripple signal imposed by the power electronics on the PV array to estimate the gradient [23]. Yet another idea is to leverage the random noise inherent to the system to estimate the gradient, similar to the stochastic perturbations that characterize certain biological processes [24].

4. Implement the proposed switched extremum seeking control system on an experimental PV array-DC/DC converter system. This could potentially be done on the PV system being installed in the new power systems laboratory.

References

[1] "Renewable Energy Cost Trends," National Renewable Energy Laboratory, Tech. Rep., 2005. [Online]. Available: http://www.nrel.gov/analysis/docs/cost_curves_2005.ppt

[2] T. Esram and P. L. Chapman, "Comparison of photovoltaic array maximum power point tracking techniques," *IEEE Transactions on Energy Conversion*, vol. 22, no. 2, pp. 439–49, 06 2007.

[3] T. Hiyama, S. Kouzuma, and T. Imakubo, "Identification of optimal operating point of pv modules using neural network for real time maximum power tracking control," *IEEE Transactions on Energy Conversion*, vol. 10, no. 2, pp. 360–7, 06 1995.

[4] T. Hiyama and K. Kitabayashi, "Neural network based estimation of maximum power generation from PV module using environmental information," *IEEE Transactions on Energy Conversion*, vol. 12, no. 3, pp. 241–7, 1997.

[5] N. Patcharaprakiti, S. Premrudeepreechacharn, and Y. Sriuthaisiriwong, "Maximum power point tracking using adaptive fuzzy logic control for grid-connected photovoltaic system," *Renewable Energy*, vol. 30, no. 11, pp. 1771–88, 2005.

[6] N. Femia, G. Petrone, G. Spagnuolo, and M. Vitelli, "Optimization of perturb and observe maximum power point tracking method," *IEEE Transactions on Power Electronics*, vol. 20, no. 4, pp. 963–973, Jul 2005.

[7] J.-M. Kwon, B.-H. Kwon, and K.-H. Nam, "Three-phase photovoltaic system with three-level boosting MPPT control," *IEEE Transactions on Power Electronics*, vol. 23, no. 5, pp. 2319–2327, 2008.

[8] K. H. Hussein, I. Muta, T. Hoshino, and M. Osakada, "Maximum Photovoltaic Power Tracking - An Algorithm for Rapidly Changing Atmospheric Conditions," *IEE Proceedings-Generation Transmission and Distribution*, vol. 142, no. 1, pp. 59–64, Jan 1995.

[9] Y. A. Chang and S. J. Moura, "Air Flow Control in Fuel Cell Systems: An Extremum Seeking Approach," *2009 American Control Conference*, 2009, St. Louis, MO, USA.

[10] J. Creaby, Y. Li, and S. Seem, "Maximizing Wind Energy Capture via Extremum Seeking Control," *2008 ASME Dynamic Systems and Control Conference*, 2008, Ann Arbor, MI, USA.

[11] K. Ariyur and M. Krstić, *Real-time optimization by extremum-seeking control.* Wiley-Interscience, 2003.

[12] G. Vachtsevanos and K. Kalaitzakis, "A Hybrid Photovoltaic Simulator for Utility Interactive Studies," *IEEE Transactions on Energy Conversion*, vol. EC-2, no. 2, pp. 227–231, 1987, iD: 1.

[13] G. Masters, *Renewable and efficient electric power systems.* John Wiley & Sons, 2004.

[14] J. G. Kassakian, M. F. Schlecht, and G. C. Verghese, *Principles of Power Electronics.* Reading, MA: Addison-Wesley, 1991.

[15] M. Krstic and H.-H. Wang, "Stability of extremum seeking feedback for general nonlinear dynamic systems," *Automatica*, vol. 36, no. 4, pp. 595–601, 04 2000.

[16] D. DeHaan and M. Guay, "Extremum-seeking control of state-constrained nonlinear systems," *Automatica*, vol. 41, no. 9, pp. 1567–1574, 2005.

[17] H. K. Khalil, *Nonlinear systems.* Prentice Hall Upper Saddle River, NJ, 2002.

[18] V. A. Caliskan, O. C. Verghese, and A. M. Stankovic, "Multifrequency averaging of DC/DC converters," *IEEE Transactions on Power Electronics*, vol. 14, no. 1, pp. 124–133, 1999.

[19] S. Bashash and N. Jalili, "Robust adaptive control of coupled parallel piezo-flexural nanopositioning stages," *IEEE/ASME Transactions on Mechatronics*, vol. 14, no. 1, pp. 11–20, 2009.

[20] D. Liberzon, *Switching in systems and control*. Birkhauser, 2003.

[21] H. Patel and V. Agarwal, "Maximum power point tracking scheme for PV systems operating under partially shaded conditions," *IEEE Transactions on Industrial Electronics*, vol. 55, no. 4, pp. 1689–98, 04 2008.

[22] Y. Tan, D. Nesic, and I. Mareels, "On the choice of dither in extremum seeking systems: A case study," *Automatica*, vol. 44, no. 5, pp. 1446–1450, 2008.

[23] T. Esram, J. W. Kimball, P. T. Krein, P. L. Chapman, and P. Midya, "Dynamic maximum power point tracking of photovoltaic arrays using ripple correlation control," *IEEE Transactions on Power Electronics*, vol. 21, no. 5, pp. 1282–1290, 2006.

[24] C. Manzie and M. Krstic, "Extremum seeking with stochastic perturbations," *IEEE Transactions on Automatic Control*, vol. 54, no. 3, pp. 580–5, 03 2009.